# Greenhouse gas emissions from stormwater bioretention basins

Emad Kavehei[*a], N. Iram[a], M. Rezaei Rashti[a], G. A. Jenkins[b], C. Lemckert[c], M. F. Adame[a]

[a]Griffith University, Australian Rivers Institute, Kessels Road, Nathan, 4111, QLD, Australia

[b]Griffith University, School of Engineering and Built Environment, Kessels Road, Nathan, 4111, QLD, Australia

[c]University of Canberra, School of Design and the Built Environment, 2617, ACT, Australia

*Emad Kavehei

Email: emad.kavehei@griffithuni.edu.au

**Abstract**

Bioretention basins are frequently subjected to anaerobic conditions, which can create an optimum environment for microbial activities to remove nitrogen (N) and sequester carbon (C) in the below-ground filter media. However, these biological processes are associated with the potential production of greenhouse gas (GHG) emissions that need to be measured. In this study, we quantified nitrous oxide ($N_2O$), methane ($CH_4$) and carbon dioxide ($CO_2$) fluxes from the soil under a transition period from dry to wet conditions in subtropical Australia. The GHG fluxes were measured on the bed of slow (wet basin) and fast (dry basin) draining basins and their embankment area. In addition, the influence of *Carex appressa* plant on emissions was investigated. Finally, the denitrification potential of the basin soil and their C and N accumulation (over an 18-month interval) were measured. The dry and the embankment soils were both slight sinks of $CH_4$ (-16 and -2 μg $CH_4$−C $m^{-2}$ $h^{-1}$) while being a high source of $CO_2$ (> 520 × $10^3$ μg $CO_2$−C $m^{-2}$ $h^{-1}$). In comparison, the wet basin was a source of $CO_2$ and $CH_4$ with a mean value of 123× $10^3$ μg $CO_2$−C $m^{-2}$ $h^{-1}$ and 2405 μg $CH_4$−C $m^{-2}$ $h^{-1}$, respectively. The dry and wet basins were a slight source of $N_2O$ emissions and were positively driven by precipitation. The presence of *C. appressa* plant increased $CH_4$ consumption and $N_2O$ generation. The results suggest that adopting a slow-draining design for bioretention systems, such as lowering the hydraulic conductivity and/or provision of a saturation zone higher in the soil profile, can reduce $CO_2$ and $N_2O$ fluxes from the soils and potentially improve water quality performance of these basins. However, an increase in $CH_4$ fluxes should be the expected by-product.

## Graphic abstract

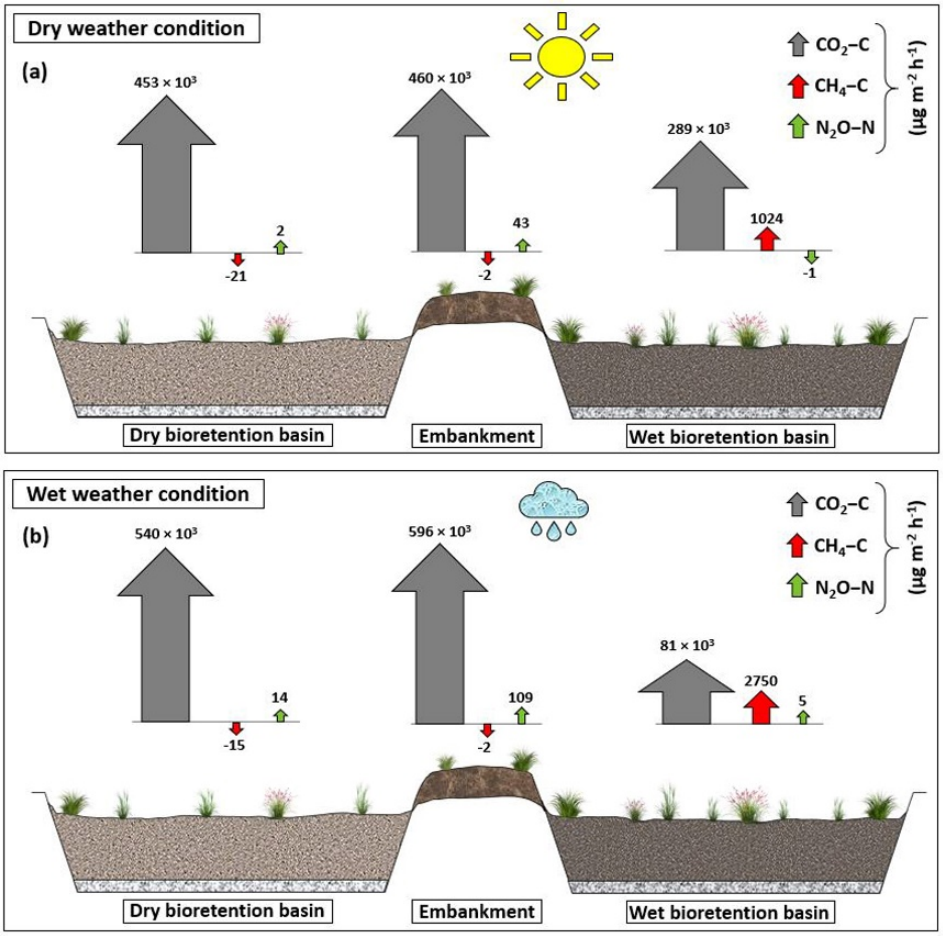


Greenhouse gas emissions (µg $m^{-2}$ $h^{-1}$) from a dry and a wet bioretention basin and their embankment area under a dry and a wet condition.


## Keywords

Green infrastructure; Stormwater control measure; denitrification potential; Water sensitive urban design systems; Global warming potential; Biofiltration basin.

## 1. Introduction

Stormwater management technologies including constructed wetlands, green roofs, swales, detention/retention ponds and bioretention basins are primarily designed for volume reduction and water quality improvement (Fletcher et al., 2015). However, they also have the potential for the provision of several ecosystem services and disservices (Vymazal, 2011). Bioretention basins are one of the most popular stormwater systems and well-known for their pollutant removal performance. These basins are engineered soil-plant ecosystems that receive stormwater runoff and gradually treat the water through the different soil sub-layers. These basins consist of a vegetated surface with specific native plants, sand-based topsoil, and drainage layers with under drainage pipes at the bottom of the basins (Hatt et al., 2009; Kavehei et al., 2018a).

Bioretention basins are designed for frequent ponding and draining. These basins have potential in accumulating nitrogen (N) and C in their filter media, which can be sequestered in the long-term through biological processes (Hatt et al., 2009; Kavehei et al., 2019). The ponding of nutrient-rich freshwater water is associated with large greenhouse gas (GHG) emissions (Ollivier et al., 2019). The main GHGs include nitrous oxide ($N_2O$), methane ($CH_4$) and carbon dioxide ($CO_2$), the former with a warming potential of 310 and 21 times more than $CO_2$, respectively (Stocker et al., 2013). From these GHGs, $CO_2$ can be produced through aerobic and anaerobic mineralisation of soil organic matter, while $CH_4$ is the product of methanogenesis under strictly anoxic conditions (Schlesinger and Bernhardt, 2013). Denitrification is one of the most important microbial processes in removing N which is the process by which nitrate ($NO_3$) is converted to $N_2O$ and $N_2$ gases, thereby improving water quality (Waller et al., 2018). The amount of $N_2O$ produced is associated with the shifts between

aerobic and anaerobic soil conditions that promote nitrification and denitrification (McPhillips and Walter, 2015; Waller et al., 2018).

There are few studies that have measured GHG fluxes on bioretention basins, mostly in temperate climates (Grover et al., 2013; McPhillips et al., 2017; McPhillips and Walter, 2015; Shrestha et al., 2018), and the influence of rainfall and changes in soil water content has not been well studied. Finally, the impact of vegetation on GHG emissions from bioretention basins has yet to be quantified. This study investigated the variation of the GHG fluxes of two bioretention basins with contrasting hydraulic conductivities of a slow (wet basin) and fast (dry basin) draining. The GHG fluxes of the two basins and their embankment area were measured during the transition from a dry weather condition to a period of rainfall. We also show the impact of the *Carex appressa* plants on soil GHG emissions in the fast-draining basin. Denitrification potential of the sites and their soil C and N accumulation over an 18-month interval were also measured to accompany the findings.

## 2. Materials and methods

### 2.1 Study sites

The study was carried out in the subtropical climate of the Gold Coast, Australia which has a warm and wet summer (November – February; 19 to 29°C) and cool and dry winter (July – August; and 12 to 21°C). The region has an average annual rainfall of 1,017 mm, with the lowest and highest average monthly rainfall of 28 mm in July and 148 mm in January (Australia Bureau of Meteorology, 2019). The GHG experiment was conducted at the two bioretention basins between the 17th September and the 20th October 2018 (Fig. 1). The basins are separated by a vegetated embankment of 3 m in

width which does not act as a pool of stormwater runoff. The two bioretention basins were built within urban areas in 2013 and designed for improving water quality with ponding areas of 1100 $m^2$ and 1180 $m^2$, respectively. The hydraulic conductivity of the basins was examined, which showed contrasting capabilities of slow (wet basin with 28 mm $hr^{-1}$) and fast (dry basin with 312 mm $hr^{-1}$) draining (see Methods below). The basins receive stormwater from an upstream catchment through separate inflow pipes. Both basins were built with an underdrain perforated pipe, while the fast-draining dry basin, was designed as a sealed basin which also transfers the outflow through three pipelines to the slow-draining wet basin. The wet basin was designed to allow infiltration of water into the surrounding soils. The vegetation of the basins was dominated by *C. appressa*, *Ficinia nodosa* and *Lomandra longifolia*, while the embankment only had *L. longifolia*.

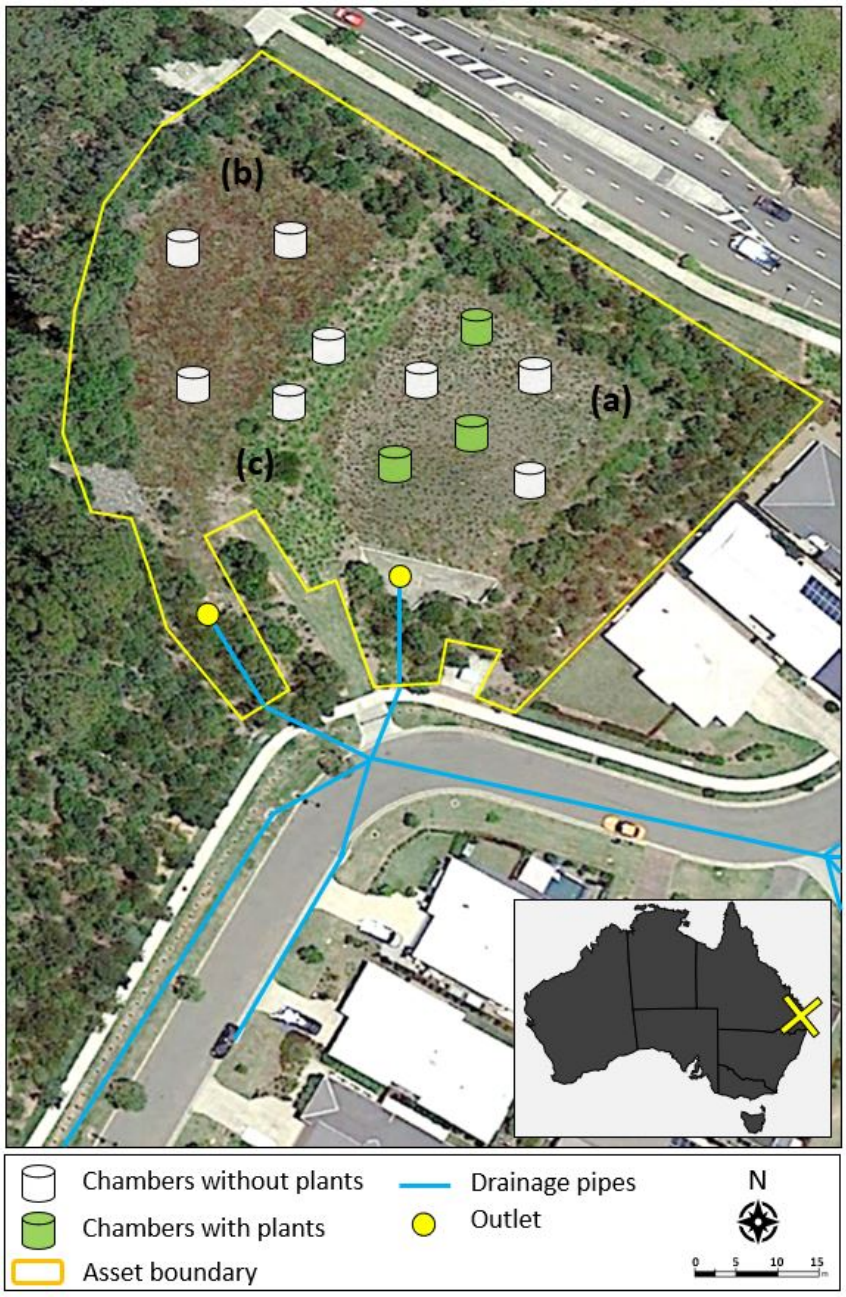


**Fig. 1.** Bioretention sites location and the position of the chambers for the GHG experiment: (a) a dry bioretention basin, (b) a wet bioretention basin, and (c) a embankment area. Site location hyperlink.

## 2.2. Soil sample collection, chemical, physical and environmental analysis

Soil cores were taken with a 40 mm-diameter open-auger (Dormer, Australia) at three points along a transect in each basin and randomly in the embankment area. The soil cores were taken at two different times within an 18-month interval, in December 2017 and July 2019. For each core, individual samples were taken at four depths of 0-5, 5-10, 10-20 and 20-30 cm. Samples of the known volume were weighted, and small subsamples were collected for pH, and total C and N analysis. The samples were oven-dried at 105˚C for 48 hours and weighted to measure the soil bulk density and water content. The subsamples of soil were oven-dried at 60˚C for 48 hours, homogenised by grinding to < 250 μm and analysed for the total C and N concentration with an elemental analyser isotope ratio mass spectrometer (EA-IRMS, Serco System, Thermo Fischer Scientific, Griffith University). The second set of samples was treated by adding 10 ml Hydrochloric acid (5.7 M) to 2.5 g soil to test for inorganic C; however, no reaction was observed for any of the samples. The soil C and N density (mg $cm^{-3}$) was calculated based on the concentration (mg $g^{-1}$) of C or N, and the soil bulk density (g $cm^{-3}$).

Soil pH analysis was performed on 10 g air-dried soil subsamples (< 2mm) using the NSW Australian standard for 1:5 soil:water suspension (Department of Sustainable Natural Resources, 2003). Soil texture was analysed for each sample using a simplified method for soil particle size analysis described by Kettler et al. (2001). In addition, the hydraulic conductivity was measured at six points, randomly distributed in the dry and wet basins following the in-situ method described by Hatt and Le Coustumer (2008). A 10 cm diameter cylinder was inserted 5 cm into the soil and was tested at two pressure heads of 5 and 15 cm of water. The level of water was maintained at the pressure heads,

and the volume of added water was recorded until infiltration was steady. Hydraulic conductivity was calculated based on the differences between the two pressure heads.

Soil temperature was recorded continuously during the 34 days of the experiment in each basin using an EL-USB-1 data logger. Probes were installed in the centre of the basins at a depth of 10 cm. Weather parameters such as daily precipitation and air temperature were monitored using a weather station located at the same elevation, 4 km from the study site (Wolffdene Alert, Bureau No.: 040761). At each event of GHG sampling, the soil water content was measured at five locations per site with the oven-drying method. Then, the water-filled pore space (WFPS) was calculated based on Equation 1 and 2. The hydroclimatic parameters of cumulative 3-day antecedent precipitation and WFPS were used to investigate the influence of precipitation on the GHG emissions.

We expected that WFPS would be influenced by antecedent rainfall over a time period longer than 3-days which represent short term influence of precipitation.

$$\text{WFPS (\%)} = \left( \frac{\text{VWC (\%)}}{(1 - \frac{\text{BD}}{2.65}) \times 100} \right) \quad (1)$$

$$\text{VWC (\%)} = \text{Gravimetric soil water content (\%)} \times \text{BD} \quad (2)$$

Where BD is the bulk density of soil (g $cm^{-3}$), and particle density were considered 2.65 (g $cm^{-3}$).

## 2.3 Denitrification

The denitrification rates of the wet and dry basins and the embankment were measured using the isotope-pairing technique (Nielsen, 1992; Steingruber et al., 2001). The method involves enriching the overlying water on the soil by $^{15}N\text{-}NO_3$ to quantify the denitrification rates from $^{15}N\text{-}N_2$ gas production. In each site, 10 cm intact soil cores (n=8) were collected with 4.8 cm diameter Perspex tubes. Eight cores were taken in each site to allow cores to be tested at three different times; 20 min ($T_0$), 2 hr ($T_2$) and 5 hr ($T_5$) after the start of the experiment. The cores were firmly capped at the bottom and were filled with the same water collected from the sites. The samples were kept standing in a large circular rack and left to equilibrate overnight. On the day after, under ambient light, the experiment started with the addition of $^{15}N\text{-}NO_3$ (Sigma-Aldrich Pty. Ltd) at a concentration of 60 µmol $L^{-1}$ to each core to (Adame et al., 2019; Nielsen, 1992). Triplicate water samples were taken from three cores before and after enrichment with $^{15}N\text{-}NO_3$ to measure dissolved nutrients. The samples were filtered through a 0.45-mm membrane filter, stored frozen and analysed for nitrate + nitrite ($NO_x^-$−N), ammonium ($NH_4^+$) and phosphate ($PO_4$) (Chemistry Centre, Department of Science Information Technology and Innovation, Brisbane, Australia).

The cores were topped up with water and capped with Perspex lids. A Teflon-coated stirr bar was suspended in each core at 3 cm above the soil and was driven by an external rotating magnet (60–70 rpm) (Cook et al., 2004). At each sampling time, 1 mL of 50% w/v Zinc Chloride ($ZnCl_2$) was added to a core and mixed throughout the water and soil to stop bacterial activity. Three 9 ml of soil-water samples were taken with a gas-tight syringe and transferred into pre-evacuated glass vials with 250 µL of the $ZnCl_2$. The vials were kept at 4º C for three days, and then the headspace gas was

analysed for $^{28}N_2$, $^{29}N_2$ and $^{30}N_2$ gases using a continuous-flow mass spectrometry (EA-IRMS, Serco System, Thermo Fischer Scientific). The denitrification rates were calculated with the following Equations described by Steingruber et al. (2001).

The rate of $^{15}NO_3^-$ denitrification ($D_{15}$) from the production rates of $r_{29}$ and $r_{30}$.

$$D_{15} = r_{29} \times 2(r_{30}) \quad (1)$$

The rate of $^{14}NO_3^-$ denitrification ($D_{14}$)

$$D_{14} = D_{15} \times \frac{r_{29}}{2(r_{30})} \quad (2)$$

Total denitrification potential in soil ($D_{total}$)

$$D_{total} = D_{15} + D_{14} \quad (3)$$

Total denitrification potential from the overlying water ($D_w^{total}$)

$$D_w{}^{total} = \frac{D_{15}}{\varepsilon} \quad (4)$$

Nitrate enrichment of $NO_3^-$ ($\varepsilon$), where a and b refer to concentrations after and before $^{15}NO_3^-$ addition.

$$\varepsilon = \left(\frac{[NO_3{}^-]_a - [NO_3{}^-]_b}{[NO_3{}^-]_a}\right) \quad (5)$$

Denitrification from the overlying water, without tracer addition ($D_w$)

$$D_w = D_w{}^{total}(1 - \varepsilon) \quad (6)$$

Coupled nitrification-denitrification in the soil ($D_n$)

$$D_n = D_{total} - D_w{}^{total} \quad (7)$$

## 2.4 GHG flux measurements

The GHG emissions measurement were conducted in ten sampling events every 2 to 6 days, designed to capture emissions before and after rainfall events. The average daily air temperature for the study period (14.6 °C to 24.5 °C) was very close to the average annual temperature (ten-year) range of 15.6 °C to 26.3 °C of the region (Australia Bureau of Meteorology, 2019). Total precipitation of 147 mm with a maximum daily record of 39 mm was recorded during the study period. The two-month records of rainfall prior to the sampling events showed only 31 mm of precipitation in total, with the maximum daily record of 7 mm, three weeks before the start of the experiment (Fig. A.1) (Australia Bureau of Meteorology, 2019). The first two sampling events before the start of rainfall can be considered as the baseline of GHG emissions for a dry condition, while the rest of the sampling events can present the variation of GHG emissions under a wet condition.

The GHG emissions were measured with the closed static chambers method. The chamber bases were installed two weeks prior to the sampling and remained in the same location throughout the experiments. The GHG emissions were quantified at three sampling locations randomly placed in the soil at points between plants in each basin and two locations on the embankment. Three chambers were installed over *C. appressa* plants within the dry basin (Fig.1). Two weeks before the start of sampling, the selected plants were cut to an equal height of 25 cm to fit in the chambers. The measurements were conducted for all sites between 9:30 to 11:00 am on the same day, reflecting the average daily temperature, and allowing for extrapolating to daily fluxes (Collier et al., 2014). It is acknowledged that in the absence of the gross primary production of plants, the values in this study only show the soil fluxes. A full carbon balance of bioretention

basins including the life cycle carbon footprint, aboveground biomass, soil C sequestration and GHG fluxes can be an area of study in future research (Kavehei et al., 2018b).

The chambers were made from white PVC pipe. The chamber bases were 24 cm in diameter and 18 cm in height with a sharp edge at the bottom which was inserted at least 6cm into the soil. Four 1.5 cm diameter holes were made in each chamber base at the two different levels of 4 and 6 cm above the soil surface to allow the flow of water. The holes were plugged with rubber stoppers before sampling. The chamber top (12 cm height) was made from PVC pipe with a rubber vent on top for gas extraction via syringe. A 10 cm width rubber band was used for sealing of the two-chamber parts.

Gas samples were collected 1 hr after the chamber closure. A 25mL syringe was inserted into the vent, and after two pumps, the sample was collected and transferred into pre-evacuated glass vials (Exetainers; Labco Ltd. UK). The ambient air samples were also collected at each site before the start of gas sampling. Additionally, gas samples were collected from a subset of three chambers at 20 and 40 min after closure to test the linearity of increases in gas concentrations. The gas samples were stored in a cool dark container and brought back to the laboratory on the same day. During the experiment, the soil temperature of each chamber was measured at the time of gas extraction with a propagation soil thermometer (Gardman, 64704) installed outside of each chamber 10 minutes before the reading. The samples were analysed for $CO_2$, $CH_4$ and $N_2O$ contents within two weeks by gas chromatography (Shimadzu GC2010 at Griffith Environmental Biogeochemistry Research Laboratory). The linear regression of the increase or decrease of the three gases with time was tested for a subset of chambers, and $R^2$ value of > 0.7 was obtained.

### 2.5 Statistical analysis

One-way analysis of variance (ANOVA) and the Tukey's honest significant difference (HSD) was used to test the differences of GHG emissions, WFPS, soil C and N among sites. Normality and homogeneity of variance were evaluated using the Shapiro-Wilk test, with significance set at 0.05. The variables were log-transformed to satisfy the assumptions of normality and homogeneity when required. The non-parametric Kruskal–Wallis test with pairwise comparison was used when the normalisation was not successful. A repeated-measures ANOVA with the Bonferroni correction was used to assess the variation of each GHG among sites. In addition, regression analysis was used to evaluate variations of each GHG with the average daily temperature of the dry and wet basin soils. The correlation of GHG fluxes with both 3-day precipitation and WFPS was reported individually. However, due to the multicollinearity between these two parameters ($p < 0.02$), the stepwise regression was used to identify the most significant parameter for multilinear regression analysis. The statistical program, SPSS (v24, IBM, New York, USA), was used for all statistical analysis and the data were presented as mean ± standard errors.

## 3. Results and discussion

### 3.1 Soil physical, chemical characteristics and environmental conditions

Soil texture of the sites ranged from loamy sand for the dry basin to sandy loam and loam for the wet and embankment sites. Soil pH was highest at the embankment area with 6.9 ± 0.03, followed by the dry and wet basins with values of 5.9 ± 0.03 and 5.6 ± 0.06 respectively. The hydraulic conductivity of the dry basin with 312 ± 21 mm $hr^{-1}$ was significantly higher than the wet basin with 25 ± 3 mm $hr^{-1}$ (Table 1;$\chi^2(1) = 8.336$,

$p = 0.004$). During the study period, the average soil temperature of the time of GHG samplings was higher in the dry basin (22.3 ± 0.3°C) compared to the wet basin (20.3 ± 0.2°C).

The wet basin had significantly higher WFPS than the dry basin and the embankment over the whole study period ($p < 0.001$). However, the WFPS of the embankment did not significantly differ from the dry basin ($p = 0.66$). The WFPS of the dry and embankment sites were highly related to the 3-day antecedent precipitation ($r = > 0.84$, $p < 0.002$), while the WFPS of the wet basin had a less significant response to the 3-day rainfall ($r = 0.71$, $p = 0.02$). The WFPS of the wet basin with a low hydraulic conductivity increased after each rainfall and reached levels of >90% during the last four events of GHG measurements.

Soil C and N were not significantly different between the two sampling dates with 18-month interval ($p > 0.2$; Fig. 2). Soil C and N accumulation was not detected during our study period ($p = 0.5$ and $p = 0.1$). The wet basin had higher soil C and N density with 16.7 ± 2.3 kg C $m^{-3}$ and 1.0 ± 0.1 kg N $m^{-3}$ compared to the dry and embankment sites with 15.1 ± 0.6 kg C $m^{-3}$ and 0.7 ± 0.0 kg N $m^{-3}$ and 15.4 ± 3.3 kg C $m^{-3}$ and 0.8 ± 0.2 kg N $m^{-3}$ respectively.

**Table 1** Physicochemical characteristics of the stormwater bioretention basins (mean ± standard error).

| Sites | Ponding Area ($m^2$) | Hydraulic Conductivity (mm $hr^{-1}$) | Soil Depth (cm) | Soil Density (g $cm^{-3}$) | pH | Soil Texture (%) | | Total C (kg C $m^{-3}$) | Total N (kg N $m^{-3}$) |
|---|---|---|---|---|---|---|---|---|---|
| | | | | | | Silt | Clay | | |
| Dry Basin | 1100 | 312 ± 21 | 0-5 | 0.9 ± 0.1 | 6 ± 0.1 | 7.3 | 4.1 | 13.4 ± 1.6 | 0.6 ± 0.1 |
| | | | 5-10 | 1.1 ± 0.2 | 5.8 ± 0.0 | 16.1 | 0.3 | 12.5 ± 1.2 | 0.5 ± 0.1 |
| | | | 10-20 | 1.3 ± 0.0 | 5.9 ± 0.1 | 7.9 | 14.3 | 14.9 ± 1.2 | 0.7 ± 0.1 |
| | | | 20-30 | 1.4 ± 0.0 | 5.9 ± 0.3 | 7.5 | 0.4 | 16.3 ± 1.5 | 0.7 ± 0.1 |
| Wet basin | 1180 | 25 ± 3 | 0-5 | 1.1 ± 0.1 | 5.5 ± 0.3 | 39.7 | 22.9 | 24.3 ± 6.9 | 1.4 ± 0.4 |
| | | | 5-10 | 1.5 ± 0.1 | 5.7 ± 0.1 | 10.0 | 59.0 | 14.7 ± 1.6 | 0.9 ± 0.1 |
| | | | 10-20 | 1.5 ± 0.1 | 5.6 ± 0.2 | 37.3 | 9.6 | 20.1 ± 3.5 | 0.7 ± 0.1 |
| | | | 20-30 | 1.5 ± 0.1 | 5.4 ± 0.6 | 22.5 | 5.1 | 11.1 ± 2.5 | 0.7 ± 0.1 |
| Embankment | | | 0-5 | 0.7 | 7.0 | 46.8 | 35.2 | 29.2 | 1.7 |
| | | | 5-10 | 0.8 | 7.0 | 35.6 | 43.2 | 14.4 | 0.8 |
| | | | 10-20 | 1.0 | 6.9 | 15.6 | 21.5 | 13.5 | 0.6 |
| | | | 20-30 | 1.2 | 6.9 | 23.5 | 11.5 | 11 | 0.5 |

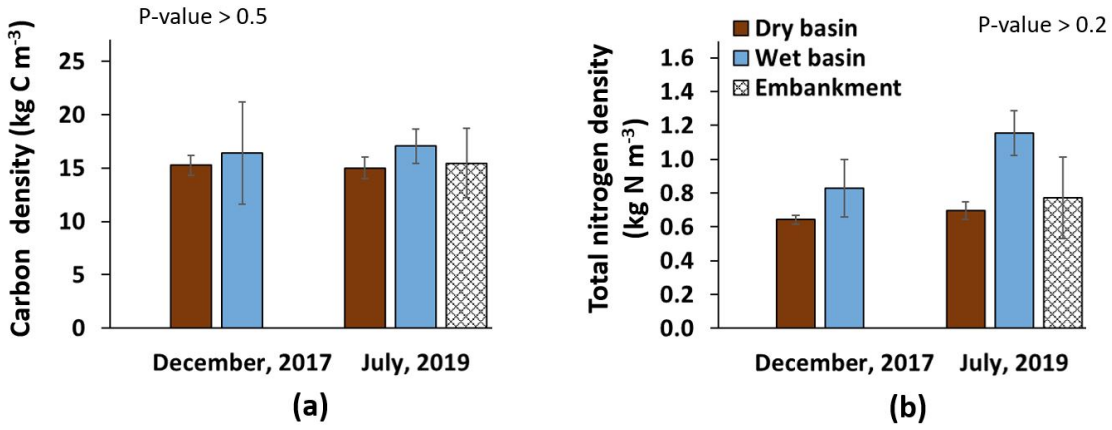


**Fig. 2.** (a) Carbon and (b) total nitrogen density (kg N $m^{-3}$) of soils in the studied sites

### 3.2 Denitrification

The mean nutrient concentrations of the water used for the experiments were 0.04 ± 0.001 mg $L^{-1}$ for $NH_4^+$−N, 0.015 ± 0.01 mg $L^{-1}$ for $NO_x^-$−N and 0.014 ± 0.001 mg $L^{-1}$ $PO_4^-$−P. When flooded, the cores with embankment soil had $NO_x^-$−N and $PO_4^-$ concentrations of 1.6 and 0.2 mg $L^{-1}$, respectively, which were higher than the samples from the dry and wet basins. The dry basin soil had higher $NO_x^-$−N and $PO_4^-$ concentrations (0.09 and 0.06 mg $L^{-1}$, respectively) compared to the wet basin (0.01 and 0.02 mg $L^{-1}$, respectively). The soil $NH_4^+$−N was highest in the dry basin, followed by the embankment and wet basin (Table 2).

Denitrification potential was lowest in the embankment and highest in the dry basin. Despite the high $NO_x^-$−N concentrations in the embankment, no denitrification could be detected (<0.01 mg N $m^{-2}$ $h^{-1}$). In the wet basin, denitrification rate was 1.0 mg N $m^{-2}$ $h^{-1}$ from which 38% originated from the water column. In the dry basin, denitrification rate was 5.3 mg N $m^{-2}$ $h^{-1}$, with 13% from the water column, and the remaining from coupled nitrification-denitrification (Table 2). The denitrification from nitrate in the water column, $D_w$ was 0.6 and 0.2 mg N $m^{-2}$ $h^{-1}$ for the dry and wet basins, respectively. The lower contribution of coupled nitrification-denitrification of the wet basin can be due to low soil $NO_x^-$−N concentrations and low oxygen penetration in the soil as the result of its low hydraulic conductivity, which limits nitrification.

Soil pH can have an impact on coupled nitrification-denitrification, as higher values move the equilibrium between ammonia ($NH_3$) and $NH_4^+$, towards high $NH_3$ and less $NH_4^+$, favouring nitrification (Nugroho et al., 2007). In our study sites, the embankment had higher pH values, which were close to neutral (6.9), while the dry and wet basin had

slightly acidic pH (5.6 and 5.9 respectively), typical of wetland conditions. The neutral soil pH of the embankment soil limited the availability of the soil $NH_4^+$ through $NH_4^+$ oxidation to $NO_x^-$−N with $N_2O$ as a by-product, while the slightly acidic soil of the dry and wet basins could have favoured $NH_4^+$ production. Kavehei et al. (2020) have shown a significant decrease in $NH_4^+$ of overlying water with an increase of the soil pH. In this current study, the dry basin had higher denitrification, as well as higher $NO_x^-$−N concentration than the wet basin. The higher $NO_x^-$−N levels in the dry basin soils could have promoted denitrification under the soil anaerobic conditions of the experiment.

A recent study on seven bioretention basins in subtropical Australia showed site age and silt content as the influencing factors on the denitrification potential of bioretention basins, ranging from 1 to 9.7 mg N $m^{-2}$ $h^{-1}$ (Kavehei et al., 2020). Studies on stormwater control measures specified that a wetter basin with longer inundation time would increase the potential denitrification (Gold et al., 2018; McPhillips and Walter, 2015). In this study, the wet basin with high soil water content and C and N availability is a potential environment for denitrification. However, very low $NO_x^-$−N concentration had limited our denitrification measurements in the wet basin. Payne et al. (2014) have shown that assimilation is the primary $NO_3$ removal fate at the low nutrient concentrations inflow and the denitrification would be at a very low rate of 0.35 mg N $m^{-2}$ $h^{-1}$. The $NO_3$ can be assimilated and stored in the soils in the form of organic compounds (Payne et al., 2014). It can be expected that at higher $NO_3$ inflow concentrations, the wet basin would have similar denitrification rates as the dry basin and will remove N through a combination of assimilation and denitrification.

**Table 2.** Denitrification and nutrient concentrations of the bioretention basins in subtropical Australia (mean ± standard error). $D_{total}$, potential total denitrification; $D_w^{total}$, total denitrification from water column; $D_w$, denitrification from nitrate from the water column; $D_n$, coupled nitrification-denitrification; ε, nitrate enrichment factor during the experiment. Nd = not detected

| Sites | **Denitrification rates** (mg N $m^{-2}$ $h^{-1}$) | | | | | **Nutrient** (mg $L^{-1}$) | | |
|---|---|---|---|---|---|---|---|---|
| | **$D_{total}$** (5h) | **$D_w^{total}$** | **$D_w$** | **$D_n$** | ε | **$NH_4^+$−N** | **$NO_x^-$−N** | **$PO_4^-$−P** |
| Dry basin | 5.3 ± 2.7 | 0.7 ± 0.4 | 0.6 ± 0.3 | 4.6 ± 2.3 | 0.13 | 0.3 ± 0.07 | 0.09 ± 0.01 | 0.06 ± 0.02 |
| Wet basin | 1.0 ± 0.4 | 0.4 ± 0.1 | 0.2 ± 0.1 | 0.6 ±0.2 | 0.38 | 0.14 ±0.03 | 0.01 ±0.0 | 0.02 ±0.0 |
| Embankment | Nd | Nd | Nd | Nd | 0.1 | 0.16 ± 0.07 | 1.59 ±0.4 | 0.22 ±0.0 |

### 3.3 GHG flux measurements

#### *3.3.1 Impact of basin types*

##### *3.3.1.1 $N_2O$*

$N_2O$ fluxes varied significantly among sites ($F_{(2,27)}$ = 37.052, $p$ = <0.0001). The wet basin fluctuated between being a sink or source for $N_2O$ and displayed significantly lower $N_2O$ fluxes than the dry basin, with mean values of 3.9 ± 2.0 µg $N_2O$−N $m^{-2}$ $h^{-1}$ and 11.7 ± 2.2 µg $N_2O$−N $m^{-2}$ $h^{-1}$ ($p$ = <0.01) respectively (Fig. 3b). Baseline emissions of -0.9 and 1.5 µg $N_2O$−N $m^{-2}$ $h^{-1}$ were estimated for the wet and dry basins, respectively. With the start of the rainfall, the $N_2O$ emissions increased to reach peak values of 14.1 and 22.8 µg $N_2O$−N $m^{-2}$ $h^{-1}$ in the wet and dry basins, respectively. The embankment had the highest values over the entire study period with a mean of 95.5 ± 18.4 µg $N_2O$−N $m^{-2}$ $h^{-1}$. The emissions from the embankment site did not show any

relationship with precipitation but increased continuously through the study period. Unlike the embankment site, the variation of $N_2O$ fluxes in both the dry and wet basins increased strongly with precipitation, as measured by both the WFPS and 3-day rainfall amount. A forward stepwise regression analysis suggested that the most influencing factor was the 3-day rainfall ($r$ = 0.85, $n$ = 10, $p$ = 0.002) for the dry basin and WFPS ($r$ = 0.68, $n$ = 10, $p$ = 0.03) for the wet basin. In addition, soil temperature did not show any influence on $N_2O$ emissions in any of the sites ($p$ = > 0.8).

The dry basin emitted more $N_2O$ than the wet basin, which can be explained by both higher denitrification and higher nutrient concentrations. Similar results have been found in temperate climates with higher $N_2O$ emissions in dry basins compared to wet basins, with 9.5 and 0.5 μg $N_2O$–N $m^{-2}$ $h^{-1}$, respectively (McPhillips and Walter, 2015). In the same study, denitrification rates and inflowing $NO_x^-$–N concentrations were higher wet basins compared with dry basins. Recent studies on stormwater control measures found that a wetter basin with longer inundation time would increase the abundance of denitrification genes and the potential for denitrification (Gold et al., 2018; McPhillips and Walter, 2015; Morse et al., 2017).

In general, WFPS of more than 50% can generate $N_2O$ emission via denitrification (Ussiri and Lal, 2012). Our results showed a significant relationship between the $N_2O$ emissions from the dry and wet basins and their soil water contents. In the dry and wet basins, the highest $N_2O$ emissions (22.8 and 14.1 μg $N_2O$–N $m^{-2}$ $h^{-1}$, respectively) were measured after a 3-day rainfall of 88 mm (WFPS of 36 % and 90 % respectively). The wet basin was a sink or very low source of $N_2O$ until the basin was submerged during the last four events of measurement with WPFS of > 90%.

The microbial reduction of $N_2O$ to $N_2$ could have happened through a complete denitrification process under anaerobic respiration of $NO_3$ or nitrite ($NO_2$) (Morse et al., 2017). In the dry basin, the switch between anaerobic and aerobic conditions could probably promote the incomplete denitrification and nitrification and subsequently produce high $N_2O$ fluxes. However, in the wet basin, the very low soil $NO_3$ could limit denitrifying bacterial activity. Morse et al. (2017) showed low soil $NO_3$ concentration in wet basins in compare to dry basins and concluded that it was due to the depletion via denitrification. In our study, the rises in the $N_2O$ fluxes from the wet basin during the last four events of GHGs sampling (92 mm rainfall) can demonstrate the denitrification potential of the basin at the presence of $NO_3$ via stormwater inflow. Overall, increased precipitation and the subsequent increased runoff, could have increased $NO_x^-$−N concentrations, which would have triggered denitrification and $N_2O$ emissions.

Bioretention basins are subjected to alternate states between ponding and draining in comparison to other aquatic systems such as constructed wetlands or stormwater ponds. This study showed that bioretention basins have low rates of $N_2O$ fluxes with an alternation between being a sink and a source of emissions which is consistent with all the published studies on bioretention basins, ranging between 0.5 to 65.6 µg $N_2O$−N $m^{-2}$ $h^{-1}$ (Table 3). In addition, stormwater ponds and basins were also a relatively low source of $N_2O$ with 4.2 and 1.8 µg $N_2O$−N $m^{-2}$ $h^{-1}$, respectively (Badiou et al., 2019; Gorsky et al., 2019). In comparison, vertical and horizontal subsurface flow and free water surface wetlands could respectively emit $N_2O$ at much higher rates with 140, 240 and 130 µg $N_2O$ −N $m^{-2}$ $h^{-1}$, respectively (Mander et al., 2014). The $N_2O$ fluxes from bioretention basins in this study are similar to those of stormwater ponds but much lower than those

of constructed wetlands. It can be concluded that it is unlikely for bioretention basins to be a significant source or sink of $N_2O$.

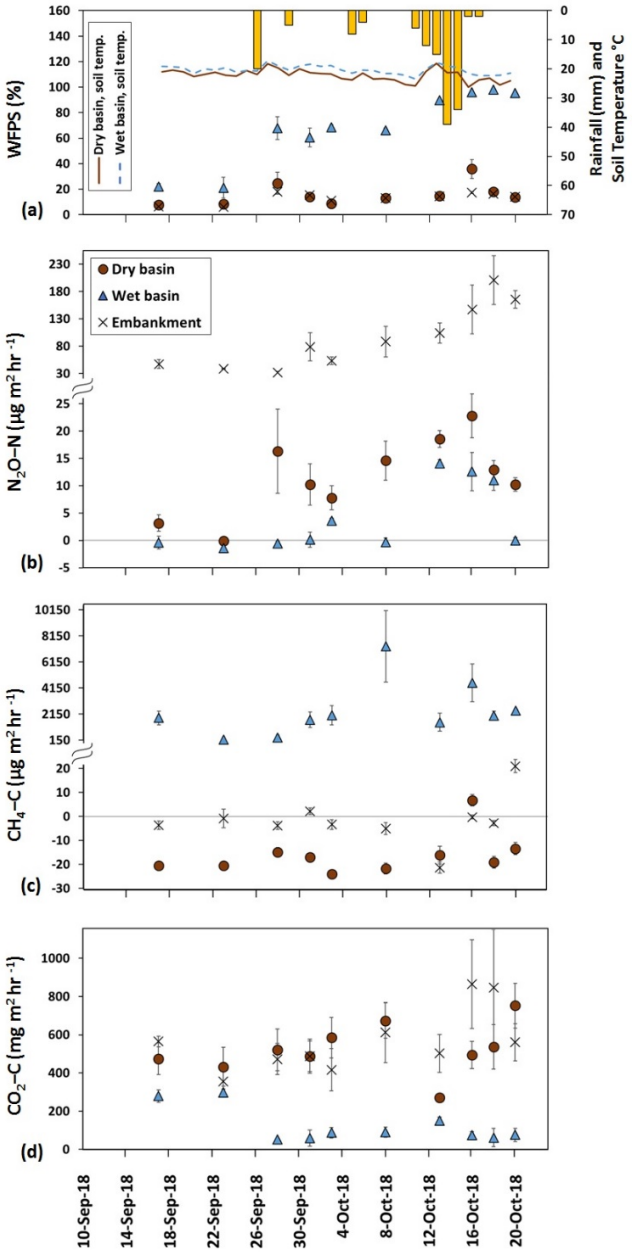


**Fig. 3.** The dry and wet bioretention basins and embankment area in subtropical Australia: (a) variation of the daily rainfall, soil water-filled pore space (WFPS) and temperature over the study period; (b) $N_2O$ fluxes; (c) $CH_4$ fluxes; (d) $CO_2$ fluxes. Positive values are emissions to the atmosphere; negative values are uptakes.

#### *3.3.1.2 $CH_4$*

The dry and embankment sites both were sinks of $CH_4$; with similar mean values of -16.1 ± 2.7 µg $CH_4$–C $m^{-2}$ $h^{-1}$ and -1.8 ± 3.2 µg $CH_4$–C $m^{-2}$ $h^{-1}$, respectively ($p$ = 0.09; Fig. 3c). Contrarily, the wet basin was a significant source of $CH_4$, with a mean value of 2405 ± 667.4 µg $CH_4$–C $m^{-2}$ $h^{-1}$, compared to the dry and embankment sites ($p$ = <0.001). A positive correlation between the $CH_4$ emissions and precipitation was found only in the dry basin, with the WFPS as the most influencing parameter ($r$ = 0.61, $n$ = 10, $p$ = 0.008). The other sites did not show any correlation with either 3-day precipitation or WFPS ($p$ = > 0.05) (Fig. A.2). Additionally, $CH_4$ emissions did not correlate with soil temperature in any of the sites ($p$ = > 0.05).

The production of $CH_4$ is the result of organic matter decomposition in anaerobic soils, which are generally waterlogged. In contrast, aerobic soils tend to be sinks of $CH_4$ as the result of oxidation (Bastviken, 2009). In bioretention basins, $CH_4$ emissions are similar to those in this study (Table 3). For instance, two bioretention basins with and without a saturated zone in temperate Australia were sinks of $CH_4$ with -16.4 and -4.2 µg $CH_4$–C $m^{-2}$ $h^{-1}$ respectively (Grover et al., 2013). McPhillips and others, studied grassed detention and bioretention basins (McPhillips et al., 2017) and the fast-draining basins (McPhillips and Walter, 2015), and also measured relatively low mean $CH_4$ flux rates of 13.1, 23.4 and -11.1 µg $CH_4$–C $m^{-2}$ $h^{-1}$ respectively.

In this study, the mean $CH_4$ emissions from the wet basin (2405 µg $CH_4$–C $m^{-2}$ $h^{-1}$) were higher than the dry basin but similar to emissions of 2756 µg $CH_4$–C $m^{-2}$ $h^{-1}$ from two wet basins in the temperate climate of the USA (McPhillips and Walter, 2015). A recent study on a complex system of bioretention basins, green roofs and bioswales also

showed similar emissions of 1900 µg $CH_4$−C $m^{-2}$ $h^{-1}$ (D'Acunha and Johnson, 2019). Although to a lower extent, the other available study on GHG fluxes from bioretention basins, also reported occasional $CH_4$ emissions of more than 100 µg $CH_4$−C $m^{-2}$ $h^{-1}$ when the soil was close to saturation (Grover et al., 2013). In our study, the basins experienced 147 mm of total rainfall over the study period, which created conditions that were close to saturation in the wet basin. This is expected to have increased the $CH_4$ emissions through mineralisation of organic C by soil microbial activity.

In this study, only the wet bioretention basin was a source of $CH_4$. However, even under very wet conditions, the wet basin showed lower $CH_4$ emission compared to other aquatic systems such as stormwater ponds (15100 µg $CH_4$−C $m^{-2}$ $h^{-1}$) (Gorsky et al., 2019) and constructed wetlands (2900 – 7400 µg $CH_4$−C $m^{-2}$ $h^{-1}$) (Mander et al., 2014). This is because bioretention basins are typically designed to have fast drainage of stormwater, which is not the case for stormwater ponds or constructed wetlands. This will tend to limit the $CH_4$ production rates in bioretention basins, especially in drier climates, such as is in subtropical Australia, when rainfall only occurs for 3-5 months of the year.

#### *3.3.1.3 $CO_2$*

$CO_2$ fluxes did not vary significantly between the dry basin and the embankment area, with the mean values of 522.5 ± 41.6 and 568.4 ± 53.3 mg $CO_2$−C $m^{-2}$ $h^{-1}$ respectively ($p$ = > 0.9). However, these emissions were significantly higher than those from the wet basin with a mean value of 122.8 ± 29 mg $CO_2$−C $m^{-2}$ $h^{-1}$ ($p$ = <0.02) (Fig. 3d). At the baseline of the experiment, the $CO_2$ flux from the wet basin was measured at 288.7± 10 mg $CO_2$−C $m^{-2}$ $h^{-1}$. With the start of the rainfall, the $CO_2$ emissions from this basin

showed a significantly negative response to the increase of soil WFPS ($r$ = -0.67, $n$ = 10, $p$ = 0.03), with a decrease to lower emission rates. The $CO_2$ fluxes from the wet basin did not correlate with 3-day antecedent rainfall ($p > 0.1$). In contrast, the $CO_2$ fluxes from the embankment site showed a significantly positive response only to the 3-day rainfall ($r$ = 0.81, $n$ = 10, $p$ = 0.004). The $CO_2$ fluxes from the dry basin did not correlate with precipitation ($p > 0.6$), and it was only the dry basin that showed a significant correlation with soil temperature ($r$ = 0.66, $n$ = 10, $p$ = 0.04)

Emissions of $CO_2$ from other bioretention basins range between 98.3 to 368 mg $CO_2$−C $m^{-2}$ $h^{-1}$ (Grover et al., 2013; McPhillips et al., 2017; Shrestha et al., 2018), (Table 3). These values are higher than our measurements in the wet basin but lower than the dry basin. Emissions of $CO_2$ and $CH_4$ are the final products of decomposition in the soil due to aerobic and anaerobic conditions, respectively (DeLaune and Reddy, 2008). The WFPS of the wet basin increased from 30 to over 90 %, which probably lead to anaerobic carbon decomposition and thus, high $CH_4$ emissions. In contrasts lower WFPS levels in the dry basin caused aerobic/anoxic mineralisation of soil organic C, resulting in high $CO_2$ emissions. The emissions from constructed wetlands (95.8 - 137 mg $CO_2$−C $m^{-2}$ $h^{-1}$) (Mander et al., 2014) tend to be higher than those of stormwater ponds (62.5 mg $CO_2$−C $m^{-2}$ $h^{-1}$) (Gorsky et al., 2019). The $CO_2$ emissions from this study were higher than both stormwater ponds and constructed wetlands.

**Table 3.** Comparison of GHG emissions from bioretention basins and similar stormwater systems. The GHG fluxes are presented in microgram of gas per square meters per hour (μg $m^{-2}$ $h^{-1}$).

| References | Basin, treatment types | $N_2O$-N | $CH_4$-C | $CO_2$-C | Vegetation | Climate |
|---|---|---|---|---|---|---|
| (Grover et al., 2013) | Bioretention, without a saturated zone | 13.8 | -4.2 | 102.2 × $10^3$ | *Carex appressa* and *Lomandra longifolia* | Mild temperate, Australia |
| | Bioretention, with a saturated zone | 65.6 | -16.4 | 98.3 × $10^3$ | | |
| (McPhillips and Walter, 2015) | Bioretention, dry basins | 9.5 | -11.1 | | *Lolium perenne* | Temperate, USA |
| | Bioretention, wet basins | 0.5 | 2756 | | *Juncus* and *Typha* | |
| (McPhillips et al., 2017) | Grassed detention basin | 13.1 | 18.9 | 198.5 × $10^3$ | *Turfgrass* | Temperate, USA |
| | Bioretention, compost-amended | 23.4 | 45.4 | 367.9 × $10^3$ | *Forsythia*, *Rosa rugosa,* and *Spiraea japonica* | |
| (Shrestha et al., 2018) | Bioretention, small roadside basins | 10 | | 194 × $10^3$ | *Native perennials plants* | Humid continental, USA |
| (D'Acunha and Johnson, 2019) | Stormwater system: bioretention, bioswale and green roof | 1.5 | 1900 | 170.8 × $10^3$ | *Typha latifolia* and *Lemna minor* | Temperate, Canada |
| This study | Bioretention, dry basin (high infiltration rate) | 11.7 | -16.1 | 522.5 × $10^3$ | *Carex appressa, Ficinia nodosa* and *Lomandra longifolia.* | Subtropical climate, Australia |
| | Bioretention, wet basin (low infiltration rate) | 3.9 | 2405 | 122.8 × $10^3$ | | |

### *3.3.2 Impact of vegetation in the dry basin*

There was a significant difference in the emissions from the chambers with and without *C. appressa* plants for $N_2O$ ($F_{(1,18)}$ = 10.238, $p$ = <0.01) and $CH_4$ ($F_{(1,17)}$ = 9.371, $p$ = <0.01). The chambers with the plants were a stronger source of $N_2O$ (26.4 ± 4.0 μg $N_2O$ −N $m^{-2}$ $h^{-1}$) and a stronger sink of $CH_4$, (-29.5 ± 3.0 μg $CH_4$−C $m^{-2}$ $h^{-1}$) compared to the chambers without plants (Fig. 4).

Oxygen diffusion through plant roots within wetlands can create an oxidised surface layer, where bacteria can facilitate $CH_4$ oxidation and consumption. In our study, the

increase in $CH_4$ consumption in the chambers with plants can be explained by an increase in oxygen due to the plant root rhizosphere, which could have promoted $CH_4$ oxidation (DeLaune and Reddy, 2008; Maucieri et al., 2017). The oxidised surface layer near the roots can also create zones of nitrification-denitrification, which can enhance $N_2O$ emissions (DeLaune and Reddy, 2008).

This study has indicated the importance of the *C. appressa* plants on GHG fluxes within bioretention basins. Although the $N_2O$ fluxes increased at the presence of plants, still the values are very small compared to constructed wetlands which are permanently ponded and can receive continuous N inputs from different sources such as wastewater, agricultural runoff and landfill leachate (Mander et al., 2014).

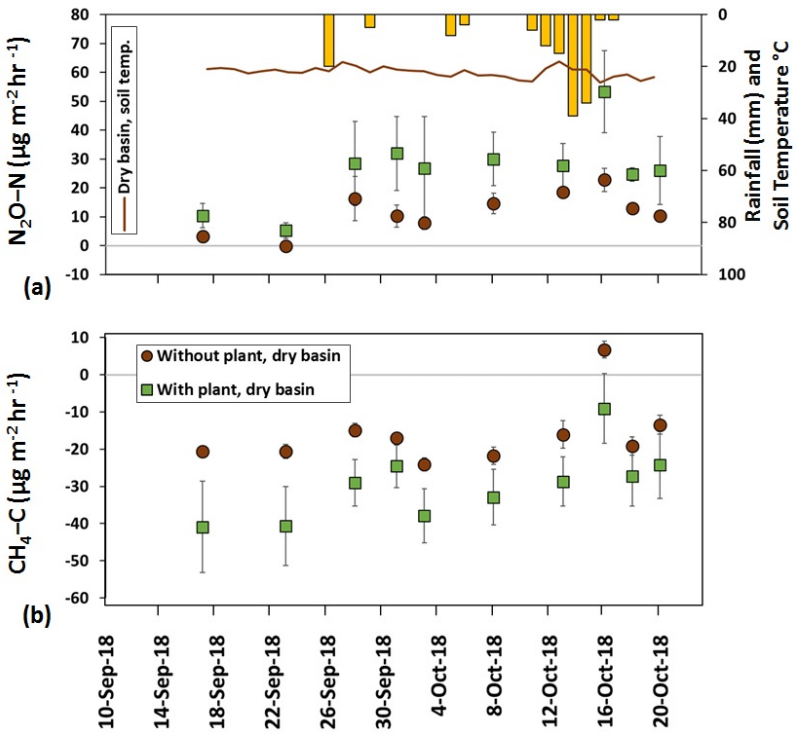


**Fig. 4.** The effects of *Carex appressa* plant within a dry bioretention basin on soil fluxes of (a) $N_2O$ and (b) $CH_4$.

### 3.4 Design implications

Overall, the soils from all sites were sources of $CO_2$, with higher emission compared to $CH_4$ and $N_2O$. This is consistent with the published literature on different bioretention basins, in which $CO_2$ fluxes from soil were the dominating GHGs (D'Acunha and Johnson, 2019; Grover et al., 2013; McPhillips et al., 2017). However, in order to have a complete $CO_2$ budget of the bioretention basins a full account on the primary production (i.e. $CO_2$ sinks) needs to be included, especially in basins with perennial or woody vegetation. This study showed that bioretention basins have relatively low rates of $N_2O$ fluxes with alternating between being a sink and a source of emissions. Bioretention basins were also a source of $CH_4$, although these emissions were lower than other water-related infrastructures such as stormwater ponds and constructed wetlands which are typically inundated for prolonged periods. These emissions need to be considered when constructing these systems.

The GHG fluxes at the baseline before the start of the rainfall were similar between the dry and wet basins. However, after the rainfall, the differences were significant; the wet basin on average emitted $460 \times 10^3$ μg $CO_2$−C $m^{-2}$ $h^{-1}$ less $CO_2$ and 2800 μg $CH_4$−C $m^{-2}$ $h^{-1}$ more $CH_4$ than the dry and embankment sites. It appears that the aerobic conditions in the dry basin and rapid changes in the soil water content trigger large $CO_2$ emissions and uptake of $CH_4$. Conversely, the low hydraulic conductivity of the wet basin allowed longer contact time with higher soil water content, which has promoted methanogenic bacteria and $CH_4$ production.

Adopting a slow-draining design for a bioretention basin with low hydraulic conductivity would increase the frequency of experiencing anaerobic conditions. This

can promote denitrification to enhance N removal from the stormwater (Gold et al., 2018; McPhillips and Walter, 2015). However, the $NO_3$ limitation could also affect this process. A fast-draining design would limit the occurrence of the anaerobic condition in the top layers of soil, where there is an abundance of organic C (Kavehei et al., 2019). This will promote aerobic respiration, and thus $CO_2$ emissions. Therefore, future bioretention basins can be designed with either a lower hydraulic conductivity, the provision of a saturation zone higher in the soil profile or including both of these features. This will increase the frequency and inundation time of anaerobic conditions after precipitations and allow minimising $CO_2$ and $N_2O$ fluxes from bioretention basins and enables to achieve higher-level treatment objectives for the basins. Although $CH_4$ would be the by-product of slow-draining design, still its $CH_4$ emissions would be lower than other water-related infrastructure such as stormwater ponds and constructed wetlands.

## 4. Conclusion

The bioretention basins were either a small sink or small source of $N_2O$, with higher emissions driven by precipitation and soil moisture. The soil of the dry basin and the embankment area were both sinks of $CH_4$ but a large source of $CO_2$. The increase in soil water content increased $CH_4$ emissions from the dry basin soil and decreased $CO_2$ emissions from the wet basin soil. The wet basin was, in general, a source of $CH_4$. The inclusion of *C. appressa* plants increased $CH_4$ uptake and $N_2O$ emissions. Both sites were sources of $CO_2$ emissions, much higher rates than those for $CH_4$ and $N_2O$. This study suggests designing wetter bioretention basins which would result in lower $CO_2$ and $N_2O$ emissions and improved nutrient removal, although $CH_4$ emissions would be the by-product of this process.

**Acknowledgement**

Gold Coast City Council for supports to this project. To the Advance Queensland Industry Research Fellowship, Queensland Government, to MFA.

**References**

Adame, M., Franklin, H., Waltham, N., Rodriguez, S., Kavehei, E., Turschwell, M., Balcombe, S., Kaniewska, P., Burford, M., Ronan, M., 2019. Nitrogen removal by tropical floodplain wetlands through denitrification. Marine and Freshwater Research 70(11), 1513-1521. https://doi.org/10.1071/MF18490.

Australia Bureau of Meteorology, 2019. Average annual, seasonal, and monthly rainfall. http://www.bom.gov.au/jsp/ncc/cdio/weatherData/av?p_nccObsCode=139&p_display_type=dataFile&p_stn_num=040761.

Badiou, P., Page, B., Ross, L., 2019. A comparison of water quality and greenhouse gas emissions in constructed wetlands and conventional retention basins with and without submerged macrophyte management for storm water regulation. Ecological Engineering 127, 292-301.

Bastviken, D., 2009. Methane, Encyclopedia of Inland Waters. Oxford: Elsevier, pp. 783-805.

Collier, S.M., Ruark, M.D., Oates, L.G., Jokela, W.E., Dell, C.J., 2014. Measurement of greenhouse gas flux from agricultural soils using static chambers. JoVE (Journal of Visualized Experiments)(90), e52110.

Cook, P.L., Revill, A.T., Butler, E.C., Eyre, B.D., 2004. Carbon and nitrogen cycling on intertidal mudflats of a temperate Australian estuary. II. Nitrogen cycling. Marine Ecology Progress Series 280, 39-54.

D'Acunha, B., Johnson, M.S., 2019. Water quality and greenhouse gas fluxes for stormwater detained in a constructed wetland. Journal of Environmental Management 231, 1232-1240.

DeLaune, R.D., Reddy, K.R., 2008. Biogeochemistry of wetlands: Science and applications. CRC press.

Department of Sustainable Natural Resources, 2003. Soil survey standard test method. Department of Natural Resources, NSW, Australia.

Fletcher, T.D., Shuster, W., Hunt, W.F., Ashley, R., Butler, D., Arthur, S., Trowsdale, S., Barraud, S., Semadeni-Davies, A., Bertrand-Krajewski, J.-L., 2015. SUDS, LID, BMPs, WSUD and more–The evolution and application of terminology surrounding urban drainage. Urban Water Journal 12(7), 525-542.

Gold, A.C., Thompson, S.P., Piehler, M.F., 2018. Nitrogen cycling processes within stormwater control measures: A review and call for research. Water research.

Gorsky, A., Racanelli, G., Belvin, A., Chambers, R., 2019. Greenhouse gas flux from stormwater ponds in southeastern Virginia (USA). Anthropocene, 100218.

Grover, S.P., Cohan, A., Chan, H.S., Livesley, S.J., Beringer, J., Daly, E., 2013. Occasional large emissions of nitrous oxide and methane observed in stormwater biofiltration systems. Science of the Total Environment 465, 64-71.

Hatt, B., Le Coustumer, S., 2008. Practice Note 1: In Situ Measurement of Hydraulic Conductivity.

Hatt, B.E., Fletcher, T.D., Deletic, A., 2009. Hydrologic and pollutant removal performance of stormwater biofiltration systems at the field scale. Journal of Hydrology 365(3-4), 310-321.

Kavehei, E., Farahani, B.S., Jenkins, G., Lemckert, C., Adame, M., 2020. Soil nitrogen accumulation, denitrification potential, and carbon source tracing in bioretention basins. Water Research, 116511. https://doi.org/10.1016/j.watres.2020.116511.

Kavehei, E., Jenkins, G., Adame, M., Lemckert, C., 2018a. Carbon sequestration potential for mitigating the carbon footprint of green stormwater infrastructure. Renewable and Sustainable Energy Reviews 94, 1179-1191. https://doi.org/10.1016/j.rser.2018.07.002.

Kavehei, E., Jenkins, G., Adame, M.F., Lemckert, C., 2018b. Towards the inclusion of greenhouse gas fluxes in the carbon footprint of vegetated WSUD, 10th International Conference on Water Sensitive Urban Design: Creating water sensitive communities (WSUD 2018 & Hydropolis 2018). Engineers Australia, Perth, Australia, p. 241.

Kavehei, E., Jenkins, G., Lemckert, C., Adame, M., 2019. Carbon stocks and sequestration of stormwater bioretention/biofiltration basins. Ecological Engineering 138, 227-236. https://doi.org/10.1016/j.ecoleng.2019.07.006.

Kettler, T., Doran, J.W., Gilbert, T., 2001. Simplified method for soil particle-size determination to accompany soil-quality analyses. Soil Science Society of America Journal 65(3), 849-852.

Mander, Ü., Dotro, G., Ebie, Y., Towprayoon, S., Chiemchaisri, C., Nogueira, S.F., Jamsranjav, B., Kasak, K., Truu, J., Tournebize, J., 2014. Greenhouse gas emission in constructed wetlands for wastewater treatment: a review. Ecological Engineering 66, 19-35.

Maucieri, C., Barbera, A.C., Vymazal, J., Borin, M., 2017. A review on the main affecting factors of greenhouse gases emission in constructed wetlands. Agricultural and Forest Meteorology 236, 175-193.

McPhillips, L., Goodale, C., Walter, M.T., 2017. Nutrient leaching and greenhouse gas emissions in grassed detention and bioretention stormwater basins. Journal of Sustainable Water in the Built Environment 4(1), 04017014. https://doi.org/10.1061/JSWBAY.0000837.

McPhillips, L., Walter, M.T., 2015. Hydrologic conditions drive denitrification and greenhouse gas emissions in stormwater detention basins. Ecological Engineering 85, 67-75.

Morse, N.R., McPhillips, L.E., Shapleigh, J.P., Walter, M.T., 2017. The role of denitrification in stormwater detention basin treatment of nitrogen. Environmental science & technology 51(14), 7928-7935.

Nielsen, L.P., 1992. Denitrification in sediment determined from nitrogen isotope pairing. FEMS Microbiology Letters 86(4), 357-362.

Nugroho, R.A., Röling, W., Laverman, A., Verhoef, H., 2007. Low nitrification rates in acid Scots pine forest soils are due to pH-related factors. Microbial Ecology 53(1), 89-97.

Ollivier, Q.R., Maher, D.T., Pitfield, C., Macreadie, P.I., 2019. Punching above their weight: Large release of greenhouse gases from small agricultural dams. Global change biology 25(2), 721-732.

Payne, E.G., Fletcher, T.D., Russell, D.G., Grace, M.R., Cavagnaro, T.R., Evrard, V., Deletic, A., Hatt, B.E., Cook, P.L., 2014. Temporary storage or permanent removal? The division of nitrogen between biotic assimilation and denitrification in stormwater biofiltration systems. PloS one 9(3), e90890.

Schlesinger, W.H., Bernhardt, E.S., 2013. Biogeochemistry: An analysis of global change. Academic press.

Shrestha, P., Hurley, S., Adair, E., 2018. Soil media CO2 and N2O fluxes dynamics from sand-based roadside bioretention systems. Water 10(2), 185.

Steingruber, S.M., Friedrich, J., Gächter, R., Wehrli, B., 2001. Measurement of denitrification in sediments with the 15N isotope pairing technique. Appl. Environ. Microbiol. 67(9), 3771-3778.

Stocker, T., Qin, D., Plattner, G., Tignor, M., Allen, S., Boschung, J., Nauels, A., Xia, Y., Bex, V., Midgley, P., 2013. IPCC, 2013: Climate Change 2013: The Physical Science Basis. Contribution of Working Group I to the Fifth Assessment Report of the Intergovernmental Panel on Climate Change, 1535 pp. Cambridge Univ. Press, Cambridge, UK, and New York.

Ussiri, D., Lal, R., 2012. Soil emission of nitrous oxide and its mitigation. Springer Science & Business Media.

Vymazal, J., 2011. Enhancing ecosystem services on the landscape with created, constructed and restored wetlands. Ecological Engineering 1(37), 1-5.

Waller, L.J., Evanylo, G.K., Krometis, L.-A.H., Strickland, M.S., Wynn-Thompson, T., Badgley, B.D., 2018. Engineered and Environmental Controls of Microbial Denitrification in Established Bioretention Cells. Environmental Science & Technology 52(9), 5358-5366.